

Zika Virus Induced Mortality and Microcephaly in Chicken Embryos

Forrest T. Goodfellow,¹ Blanka Tesla,² Gregory Simchick,³ Qun Zhao,³ Thomas Hodge,² Melinda A. Brindley,⁴ and Steven L. Stice⁵

The explosive spread of the Zika virus (ZIKV) through South and Central America has been linked to an increase in congenital birth defects, specifically microcephaly. Representative rodent models for investigating infections include direct central nervous system (CNS) injections late in pregnancy and transplacental transmission in immunodeficient mice. Microcephaly in humans may be the result of infection occurring early in pregnancy, therefore recapitulating that the human course of ZIKV infection should include normal embryo exposed to ZIKV during the first trimester. In ovo development of the chicken embryo closely mirrors human fetal neurodevelopment and, as a comparative model, could provide key insights into both temporal and pathophysiological effects of ZIKV. Chick embryos were directly infected early and throughout incubation with ZIKV isolated from a Mexican mosquito in January 2016. High doses of virus caused embryonic lethality. In a subset of lower dosed embryos, replicating ZIKV was present in various organs, including the CNS, throughout development. Surviving ZIKV-infected embryos presented a microcephaly-like phenotype. Chick embryos were longitudinally monitored by magnetic resonance imaging that documented CNS structural malformations, including enlarged ventricles (30% increase) and stunted cortical growth (decreased telencephalon by 18%, brain stem by 32%, and total brain volume by 18%), on both embryonic day 15 (E15) and E20 of development. ZIKV-induced microcephaly was observed with inoculations of as few as 2–20 viral particles. The chick embryo model presented ZIKV embryonic lethal effects and progressive CNS damage similar to microcephaly.

Keywords: Zika, microcephaly, embryo

Introduction

THE EMERGENCE OF the Zika virus (ZIKV) in Central and South America has garnered global interest as increasing epidemiological data suggest a concordance between ZIKV infections and microcephaly, which is a congenital birth defect characterized by a small head and brain development deficits [1]. Since the onset of the contemporary ZIKV epidemic, the scientific community has been working quickly to understand the progression of ZIKV-induced central nervous system (CNS) malformations. Although substantial scientific effort has been directed to curb the transmission of ZIKV, significant gaps in understanding the pathophysiology and virology remain.

Our goal was to explore a novel in vivo model for ZIKV-induced brain damage that will compliment and address

limitations in current in vivo mammalian model systems. Historically, chick embryos have been extensively used in developmental biology, teratology, and virology studies [2–4]. Little is known about ZIKV infection in whole chick embryos and available information dates back to 1976, where ZIKV did not infect chicken embryonic cells in culture (monolayers and suspension) [5]. Embryonated hen eggs have been proven useful in other viral cultures due to the fact that they are large in size, low cost, and could have a higher throughput for therapeutic testing than other in vivo models. A chick embryo model could prove advantageous in a time of scientific uncertainty surrounding ZIKV pathophysiology.

Chick embryos were permissive to ZIKV infection, and progressive ZIKV-induced brain malformations occur after

¹Department of Animal and Dairy Science, Interdisciplinary Toxicology Program, Regenerative Bioscience Center, College of Agriculture and Environmental Science, University of Georgia, Athens, Georgia.

²Department of Infectious Diseases, College of Veterinary Medicine, University of Georgia, Athens, Georgia.

³Bioimaging Research Center and Department of Physics and Astronomy, University of Georgia, Athens, Georgia.

⁴Department of Infectious Diseases, Population Health, Center for Vaccines and Immunology, College of Veterinary Medicine, University of Georgia, Athens, Georgia.

⁵Department of Animal and Dairy Science, Regenerative Bioscience Center, College of Agriculture and Environmental Science, University of Georgia, Athens, Georgia.

early ZIKV infection. This work established an inexpensive, well-studied, nonimmunocompromised *in vivo* animal model capable of recapitulating the teratology of ZIKV infections. Importantly, the chick embryo model affords the opportunity to study advanced development of the CNS, beyond the embryo stages previously reported in mammalian models [6,7]. The chick embryo model provides potentially higher throughput, automated egg injection techniques are routine, and could open up the use of tens of thousands of ZIKV-embryonated eggs per hour in future ZIKV therapeutic screening campaigns [8,9].

Materials and Methods

ZIKV strain—Zika virus isolate MEX1-44 was obtained from the University of Texas Medical Branch (UTMB) Arbovirus Reference Collection. The isolate was collected from a field-caught *Aedes aegypti* mosquito from Chiapas, Mexico, in January 2016 [10]. The virus was passaged four times in Vero cells at UTMB, and an additional two times at the University of Georgia (UGA). All infections were completed using pass six stock. The virus stock was sequenced with Sanger sequencing and found to be 99% identical to the Brazilian isolates obtained from microcephaly cases [11]. Complete phylogenetic analysis is summarized by Guerbois et al. [10].

ZIKV infection—A common protocol used in developmental biology for avian embryo manipulations was minimally altered to suit our application [12]. Briefly, embryonated broiler eggs (obtained from the UGA Poultry Science Farm) were set in a standard egg incubator at 37°C and 50%–60% humidity and inoculated on either embryonic day 2.5 (E2.5) or embryonic day 5 (E5). After sterilizing with ethanol and reinforcing the shell with clear tape, three milliliters of albumen was removed and the eggshell was windowed to visualize the embryo. Virus was injected through the amniotic membrane using a glass capillary tube drawn into a needle. Two microliters of Dulbecco's modified Eagle medium (DMEM) containing no, 0.2, 2, 20, 200, 2,000, or 20,000 viral particle forming units was administered within the inner membrane space with the Picospritzer III (Parker Hannifin Corp.). Eggs were sealed with hot glue and a glass coverslip, and immediately returned to the incubator.

Quantification of Viral Load—The number of infectious ZIKV particles was monitored with plaque assays (infection was confirmed by quantitative reverse transcriptase PCR, data not shown). The embryo, extraembryonic tissue, and yolk/albumin material were collected from less than 10-day-old embryos and individual organs were dissected from older embryos. Each of the tissues was weighed and homogenized with stainless steel beads and 1 mL of DMEM in a QIAGEN TissueLyzer. The solid material was removed through centrifugation (20,000g, 5 min) and the cleared material was titered. Vero cells were infected with 10-fold serial dilutions of sample for 1–2 h. The inoculum was then removed, replaced with semisolid agar overlay, and the cells were incubated for 4–5 days at 37°C, 5% CO₂. The cells were fixed in formalin, stained with crystal violet, and the number of viral plaques was enumerated.

Magnetic resonance imaging (MRI) of chicken embryos—All MRI experiments were carried out on a 7 T Varian Magnex small animal scanner with a maximum gradient strength of 440 mT m⁻¹. Chicken embryos were scanned

with MRI at two time points (E15 and E20 of chick embryo development), and eggs were chilled at 4°C for one hour before imaging. Embryos were immediately returned to the incubator after imaging on E15 and humanly euthanized by decapitation after imaging on E20.

Both T₁-weighted and T₂-weighted anatomical images were acquired using the following protocol: T₁-weighted fast spin echo sequences (TR = 1.1 s, effective TE = 28.5 ms, FOV = 60 × 60 mm², image matrix = 256 × 256, 16–22 slices depending on embryonic day, thickness = 1 mm) and T₂-weighted fast spin echo sequences (TR = 4–6 s depending on number slices, effective TE = 112 ms, FOV = 60 × 60 mm², image matrix = 256 × 256, 16–22 slices depending on embryonic day, thickness = 1 mm). Quantitative magnetic resonance (MR) relaxation time T₂s was estimated using in-house Matlab programs, where data were acquired by multiecho, multislice spin echo sequences (TR = 3–4.5 s depending on number slices, TE = 15 ms, number of echoes = 12, FOV = 60 × 60 mm², image matrix = 256 × 256, 16–22 slices depending on embryonic day, thickness = 1 mm). Investigators were blinded to all MR images for volumetric characterization with ImageJ's ROI tool.

Statistics—All analyses were conducted in R (A Language and Environment for Statistical Computing). MRI volumetric measurements were compared by ANOVA. A *P*-value of <0.05 indicated statistically significant differences between groups.

Biosafety—All studies were conducted in accordance with NIH and UGA guidelines for embryonated chicken eggs. All virus work was approved by the UGA's institutional biosafety committee.

Results

Chick embryos are permissive for ZIKV infection

Embryonated broiler eggs were infected with ZIKV MEX1-44, a strain isolated from a field population of Mexican mosquitoes in January 2016 [10]. Eggs were inoculated with an amniotic injection of ZIKV on embryonic day 2.5 (E2.5) or embryonic day 5 (E5), accomplished with an established windowing procedure to access the embryo [12]. Daily monitoring of embryo viability showed dose-dependent mortality three days following infection. To determine if ZIKV replication was occurring in the chick embryos, a proportion of the embryos was harvested 3 days postinfection (dpi) and the presence of infectious ZIKV particles was monitored with plaque assays. The percentage of the population exhibiting ZIKV replication was dose dependent after both E2.5 and E5 infections (Fig. 1A).

The number of infectious viral particles, harvested from each embryo, was at least 100-fold greater than the inoculum, confirming active virus replication (Fig. 1B). In addition, chick embryos that were confirmed to contain active ZIKV infections (ZIKV⁺) showed dramatic mortality within 3 dpi, and only embryos exposed to the three lowest doses of ZIKV survived to embryonic day 20 (E20) of *in ovo* development (Fig. 1C). In data not shown, a small group of embryos was infected on embryonic day 13 (E13) and active ZIKV infection was identified 7 dpi on E20, yet no fetal mortality was observed.

The presence of virus observed at the end of *in ovo* development was not significantly altered by the day of ZIKV

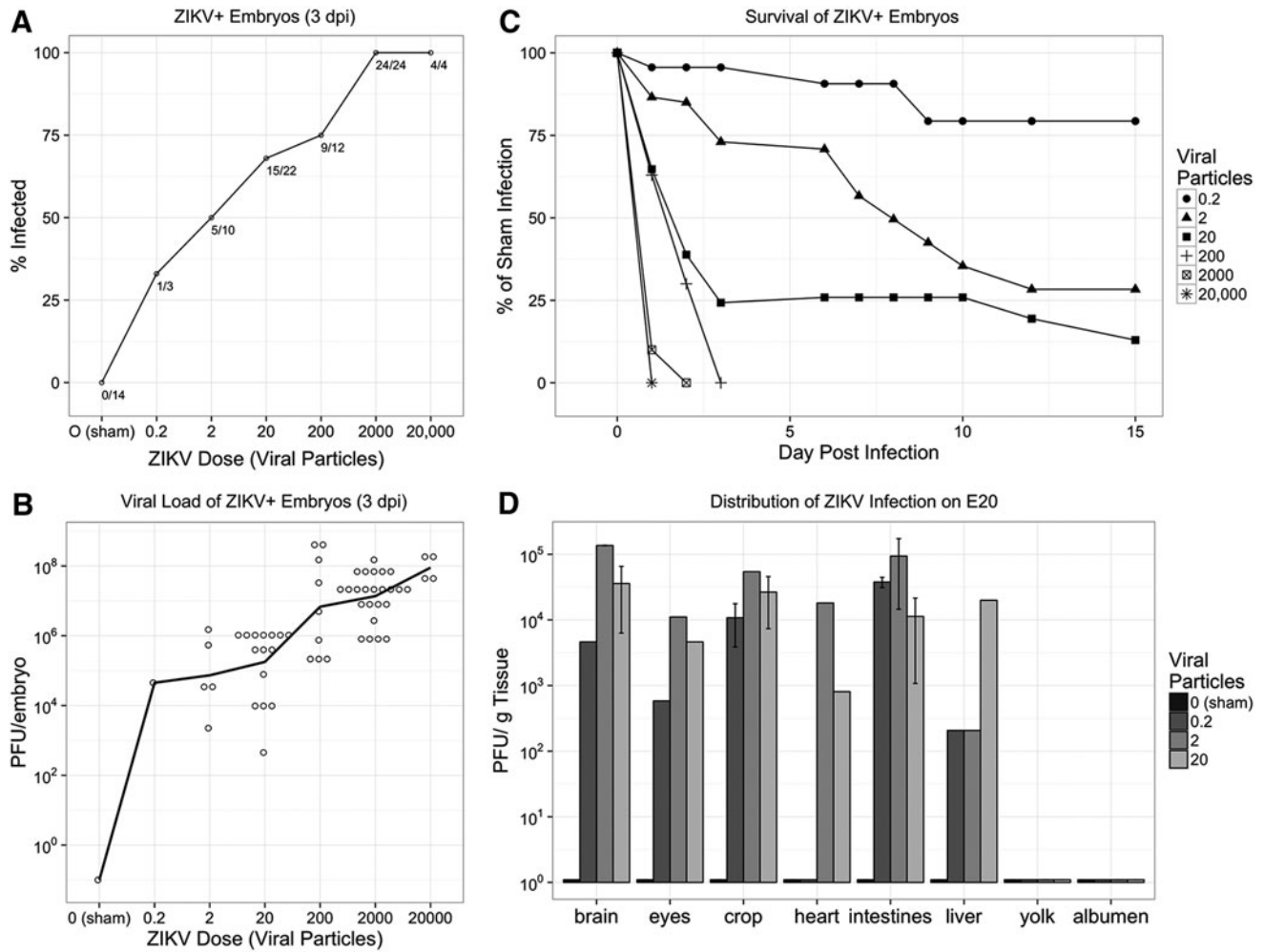


FIG. 1. The chick embryo is permissive to persistent ZIKV infection in all organs and causes embryo death. **(A)** At 3 days postinfection (dpi), chick embryos display a proportional increase in infectivity to ZIKV infection. As few as 0.2 viral particles were sufficient to infect embryos, but infection rates increase with greater numbers of viral particles. **(B)** ZIKV-positive (ZIKV⁺) embryos display active viral replication. At 3 dpi, the viral load in ZIKV⁺ embryos dramatically increased from the initial injected dose. *Open circles* indicate individual observations, and *line* indicates the mean of each dose. **(C)** ZIKV⁺ chick embryos demonstrate dose-dependent survival with high mortality within the first 3 dpi. **(D)** Infectious viral particles were isolated from E20 chick embryos after infection—substantial viral loads were identified within the brain, eyes, and all other tissues evaluated relative to 0 particles (sham) injection. ZIKV, Zika virus.

infection or the narrow dose level, and therefore results for these treatment groups were pooled for all subsequent endpoints. High viral loads were consistently identified within the brain and eyes of E20 chick embryos (Fig. 1D). Beyond the CNS, high viral loads were observed in the crop, heart, intestine, and liver (Fig. 1D). The widespread distribution of replicating ZIKV particles in multiple organs suggests that initial low-level infection of ZIKV can lead to persistent viral growth in the chick embryos. The embryos were not perfused before organ harvest and at least some of the virus observed in the various tissues may have been circulating in the blood.

In vivo imaging of Zika-induced brain damage

ZIKV-induced brain neuropathology was observed using magnetic resonance imaging (MRI). Chick embryos were imaged on embryonic day 15 (E15) and E20 of development. Eight sham-injected embryos and 12 ZIKV-infected

embryos were imaged. MR imaging slices were oriented to keep bilateral symmetry on the head, by checking the appearance of the two eyeballs. Two of the 12 ZIKV-infected embryos displayed gross defects on anatomical T₂-weighted MR images at E20 (Fig. 2A). Hyperintensity or bright contrast shown in the inset box of ZIKV-infected chick embryos indicates higher content of fluid in the malformed brain area.

Segmentation of anatomical MRI afforded volumetric quantification of specific brain regions. When comparing uninfected and infected embryos, volumetric quantification revealed stunted CNS growth between E15 and E20 in ZIKV-infected embryos (Fig. 2B–F). Noninfected embryos demonstrated a significant increase in whole brain volume and within all cortical brain regions from E15 to E20 (Fig. 2B–D). Conversely, ZIKV infections stunted the growth of the chick embryo CNS as evident by nonsignificant increases in brain volume with only the cerebellum exhibiting significant growth, while other cortical regions remained undersized. We observed

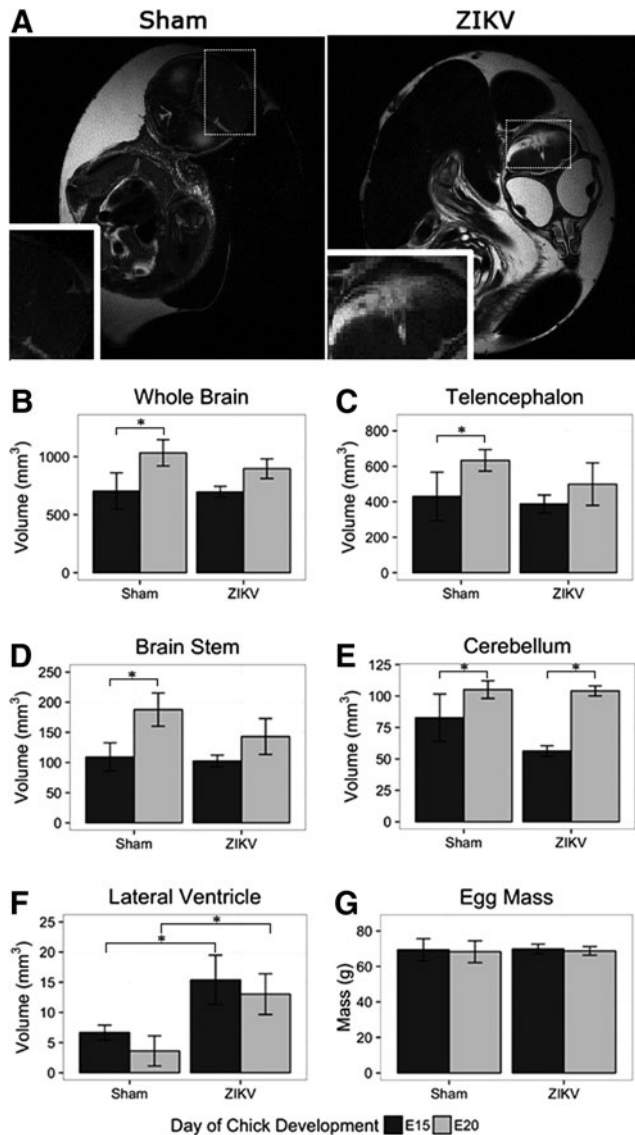


FIG. 2. MRI reveals that ZIKV-infected chick embryos have stunted brain growth. (A) Anatomical MRI T_2 -weighted images show integrity of sham-injected chick embryo telencephalon (left) and malformation in similar region of ZIKV-infected chick embryo (right). Dashed boxes represent location of inset images. (B) The whole brain, (C) telencephalon, and (D) brain stem demonstrate significant increase in volume from E15 to E20, while ZIKV-infected embryos did not. (E) The growth of the cerebellum did not appear to be stunted, and (F) the lateral ventricles of ZIKV-infected embryos were significantly increased at both E15 and E20 when compared to DMEM-injected control embryos. (G) The difference in mass of DMEM-injected control eggs and ZIKV-infected eggs was negligible. All comparisons were made with one-way ANOVA, $*P < 0.05$. DMEM, Dulbecco's modified Eagle's medium; MRI, magnetic resonance imaging.

a decreased growth of total brain volume (-18%), telencephalon (-18%), and brain stem (-32%) (Fig. 2B–D). In addition to decreased cortical volume, ZIKV-infected chick embryos presented enlarged ventricular space ($+30\%$) compared to sham injected (Fig. 2F).

When comparing the sham-injected to ZIKV-injected embryos at day 20, the virally infected embryos displayed smaller whole brain volume, telencephalon, and brain stem, although the decrease was not significant (Fig. 2B–D). The infected embryos did display a significant increase in lateral ventricle volume (Fig. 2F). The smaller total brain volume in combination with the significantly larger ventricles suggest that the ZIKV-infected embryos had less cortical tissue compared to sham-injected controls.

Previously, MR relaxation time T_1 and T_2 maps were used to longitudinally monitor developmental study of chick embryos, and the T_2 maps specifically provided insights into developing pathology changes [13]. The T_2 values of comparable brain regions of ZIKV-infected embryos increased (Fig. 3A). A distribution of T_2 values of ZIKV-infected brain area reveals a shift toward the higher end (Fig. 3B). Higher T_2 s suggest more fluid in the ZIKV-infected brain area, which is consistent with the hyperintensity contrast in the same area of anatomical images (Fig. 2A). Unlike the T_2 -weighted MR images and quantitative T_2 maps, T_1 -weighted MR images of the same ZIKV-infected embryos did not show clear brain malformation (Fig. 4). These suggest limited or no calcification formation associated with necrosis in ZIKV-infected embryos after 17.5 or 15 dpi [14,15].

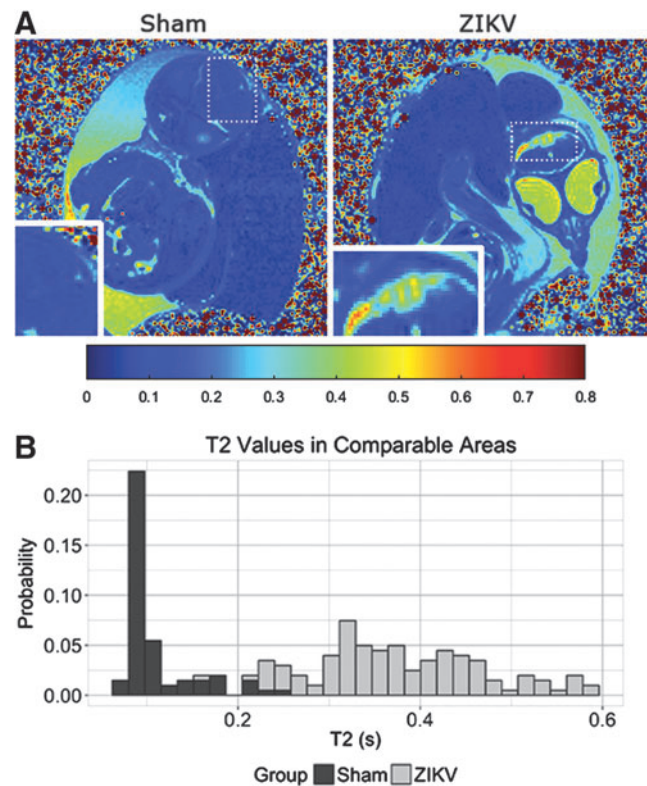


FIG. 3. ZIKV infection leads to altered T_2 contrast. (A) Quantitative MRI T_2 maps calculated from acquired SEMS images demonstrate the changes between sham-injected embryos (left) and ZIKV (right) at E20. Higher T_2 s suggest more fluid in the ZIKV-infected brain area, which is consistent to the hyperintensity contrast in the same area of anatomical images (Fig. 2A). Dashed boxes represent location of inset images. (B) T_2 quantification of comparable brain areas indicated ZIKV infections increases T_2 values, and the histogram depicts these changes.

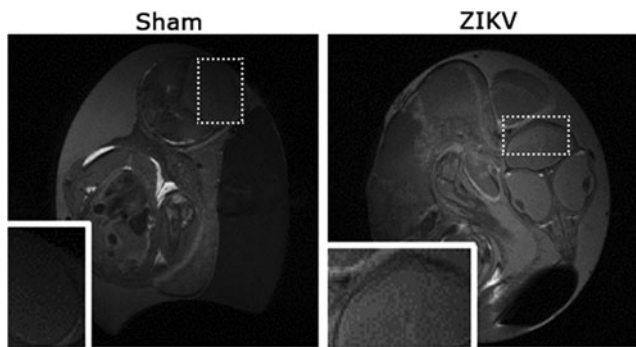


FIG. 4. Anatomical T_1 -weighted MRI images (Sham: *left*, ZIKV infected: *right*) of the same embryos as in Fig. 2. The ZIKV-infected brain did not seem to show signs of calcifications. *Dashed boxes* represent location of *inset* images.

Discussion

Prior chicken studies suggested that chick cells could not be infected with ZIKV; however, we were able to show that chick embryos were susceptible and permissive to ZIKV infection [5]. Furthermore, high-dose ZIKV infection resulted in chick embryo loss, while low doses led to sustained viral infection through development. High viral loads were identified within the brain and eyes of chick embryos, indicating that ZIKV shared cytotropism for chick CNS tissues, infection of tissues similar to human clinical pathophysiology, and parallel findings in human neural cells and in vivo murine model systems [16–18]. In vivo models would allow for further extrapolation of sustained high viral infection loads to structure function relationships in an organized CNS.

Human clinical data suggest that embryonic mortality observed may diminish if ZIKV infection occurs later in development [19]. In this study, ZIKV inoculations were conducted on E2.5 and E5 of chick embryonic development at the time of early neurogenesis [20]. ZIKV doses above 20 viral particles led to significant embryonic lethality within 3 dpi at both E2.5 and E5. Since embryonic lethality was dose dependent, future mechanistic studies may require careful dosing of the ZIKV. We hypothesize that ZIKV developmental malformations may be dose, level, and replication dependent. Also, we observed no embryo mortality when infection occurred later in chick development (E13), underscoring the benefits of in vivo models that can be infected early in development with ZIKV infection progressing over several weeks. Differential susceptibility to timing and dose of ZIKV remains to be understood during human pregnancy, and these questions could be refined and narrowed with a chick ZIKV embryo model.

Epidemiological findings report greater risk of microcephaly when mothers have an active ZIKV infection during the first trimester of pregnancy [21]. ZIKV infection can also lead to fetal mortality and a spectrum of developmental abnormalities in humans, and the underlying cause is unknown [22]. The chick embryo model provided the opportunity to study ZIKV infection from early neurogenesis throughout CNS maturation [20]. Further studies will elucidate the cell types initially infected, likely neural progenitor cells, and the ultimate fate of these cells [6,18]. The neurodevelopmental maturity of the embryonic day 21 (E21) chick embryo en-

compassed the entirety of mouse gestation and an additional 14 days of postnatal mouse development [23]. Chick embryogenesis more closely mirrors human neural developmental when compared to postnatal day 0 mouse pups. Also, higher levels of multivariable treatment groups are not easily generated in mammalian in vivo models. Consequently, a chick embryo in vivo model that is relatively fast, inexpensive, and amenable to high-throughput systems could address these gaps.

A striking aspect of ZIKV infection is the progressive congenital birth defects observed, namely microcephaly [6,24]. The chick embryo model facilitated longitudinal MRI observations, a significant benefit for a chick ZIKV model [25]. MRI observation could provide insight into the timing and anatomical location of brain malformations. We conducted MRI at E15 and E20 (Fig. 2). The chicken embryo demonstrated progressive changes in ZIKV-induced brain region volume that was observed across all cortical regions except the cerebellum, and was accompanied by increased ventricular volumes. These observations are in agreement with human clinical observations reported from regions with prevalent ZIKV infection, where ventriculomegaly has also been reported [11,26]. Mouse studies have reported the opposite, finding ZIKV infection resulted in smaller lateral ventricles and a decrease in ventricular surfaces [27].

T_2 -weighted MR images demonstrate brain damage in the developing chick CNS (Fig. 3A). Higher T_2 values suggest more fluid in the ZIKV-infected brain area, which was consistent to the hyperintensity contrast in the same area of anatomical images (Figs. 2A and 3A). In clinical studies, T_1 -weighted images have suggested calcification of brain tissues [14,15]. Although calcification was not observed in this study, timing of initial infection and duration thereafter might be a factor and should be further examined in the future. In addition, there are some limitations to this study. For example, MRI of chick embryos needs to be completed along certain orientations so that similar slices can be used for comparison between ZIKV-infected and sham embryos. Chilling of embryos at 4°C for 1 h before imaging was adopted to reduce motion of embryos during a scan, but a double-oblique imaging orientation (eg, parallel to the beak while going through two eyeballs symmetrically) should be sought in future studies.

The first animal mammalian models of ZIKV-induced brain damage have recently been reported and provide key insights into the pathophysiology of ZIKV [16,28]. Non-human primate models are likely to be the most representative of human infections, but they are arduous, lengthy, and expensive studies [29]. In addition, although only a couple of pregnant animals have been infected, currently no signs of brain damage or virus-induced damage have been described in the rhesus model (Zika.labkey.com). Mouse models have been more successful in replicating transplacental virus replication [24,30]. All mouse models report substantial intrauterine growth restriction, resulting in small pups, making specific microcephaly more challenging to define. Unlike the mouse, we did not find a decrease in gross ZIKV-infected embryo size when compared to sham-injected controls. In the future, it may be possible to develop ZIKV chick embryos having CNS-specific developmental deficiencies, without altering other organ systems.

ZIKV infections in the pregnant mouse can require immunocompromised lines and have a limited window of

prenatal CNS development for exposure. The most recent study demonstrating transplacental spread of ZIKV produced infected embryos 10 days postfertilization [24]. While this is the earliest reported infection in the mouse model that resulted in full-term pups, it only permits the virus to be present for 10 days of fetal development, whereas the chick embryo model facilitates ZIKV infections in excess of 15 days. Mouse transplacental infections earlier during development have resulted in embryo loss [7].

Additional groups have bypassed infecting the mother, and directly infect the developing mouse brain [6]. Because mouse embryos are small in size, it would be technically difficult to directly expose fetal tissue *in vivo* to ZIKV early in pregnancy, and these studies were performed on older E13.5 embryos [6]. Consequently, only later stage mouse embryos have been directly injected with ZIKV, which is later than the corresponding first trimester pregnancy in humans, when it is thought that most human infections occur [21,24]. Therefore alternative models and *in vitro* systems may provide insight into the timing and underlying mechanism of ZIKV damage, including microcephaly, and will likely provide additional systems for developing diagnostic platforms and therapeutics [31].

In summary, the chick embryo was both permissive to ZIKV infection, vulnerable to ZIKV-related mortality, and exhibited ZIKV-induced brain changes and likely damage. These attributes are fundamental to the ZIKV pathology observed in humans and now avail the chick embryo model as a viable alternative model organism. Therapeutic screening campaigns to mitigate ZIKV infection, reduced growth in fetal organs, including the CNS, as well as reduced early embryo mortality can now be monitored in a traditional developmental biology model with relatively higher throughput, potentially upward of 10,000 eggs injected per hour. The chick embryo offers an alternative and complimentary animal model for studying ZIKV pathogenesis.

Acknowledgments

We thank Dr. Robert Beckstead and Dr. Jeanna Wilson of the UGA Poultry Science Department for assistance procuring embryonated broiler eggs. This work was supported, in part, by U.S. Environmental Protection Agency STAR grant (83555101), National Science Foundation under the Science and Technology Center, and grant S10RR023706 from the National Center for Research Resources.

Author Disclosure Statement

No competing financial interests exist.

References

- Schuler-Faccini L, EM Ribeiro, IM Feitosa, DD Horovitz, DP Cavalcanti, A Pessoa, MJ Doriqui, JI Neri, JM Neto, et al; Medical Genetics Society-Zika Embryopathy Task. (2016). Possible Association Between Zika Virus Infection and Microcephaly - Brazil, 2015. *MMWR Morb Mortal Wkly Rep* 65:59–62.
- Drake VJ, SL Koprowski, JW Lough and SM Smith. (2006). Gastrulating chick embryo as a model for evaluating teratogenicity: a comparison of three approaches. *Birth Defects Res A Clin Mol Teratol* 76:66–71.
- Hamburger V and HL Hamilton. (1992). A series of normal stages in the development of the chick embryo. 1951. *Dev Dyn* 195:231–272.
- Woodruff AM and EW Goodpasture. (1931). The susceptibility of the chorio-allantoic membrane of chick embryos to infection with the fowl-pox virus. *Am J Pathol* 7:209–222 205.
- Way JH, ET Bowen and GS Platt. (1976). Comparative studies of some African arboviruses in cell culture and in mice. *J Gen Virol* 30:123–130.
- Li C, D Xu, Q Ye, S Hong, Y Jiang, X Liu, N Zhang, L Shi, CF Qin and Z Xu. (2016). Zika virus disrupts neural progenitor development and leads to microcephaly in mice. *Cell Stem Cell* 19:120–126.
- Miner JJ, B Cao, J Govero, AM Smith, E Fernandez, OH Cabrera, C Garber, M Noll, RS Klein, et al. (2016). Zika virus infection during pregnancy in mice causes placental damage and fetal demise. *Cell* 165:1081–1091.
- Avakian AP, PS Wakenell, T Bryan, JL Schaeffer, CJ Williams and C Whitfill. (2002). *In ovo* administration of Marek's disease vaccine: importance of vaccine deposition site in the fertile egg. In: *51st Western Poultry Disease Conference*, Puerto Vallarta, Mexico.
- Barbosa T, C Williams and T Villalobos. (2013). Efficacy and Marek's disease protection comparison between different vaccination methods. In: *18th Congress World Veterinary Poultry Association*, Nantes, France.
- Guerbois M, I Fernandez-Salas, SR Azar, R Danis-Lozano, CM Alpuche-Aranda, G Leal, IR Garcia-Malo, EE Diaz-Gonzalez, M Casas-Martinez, et al. (2016). Outbreak of Zika virus infection, Chiapas State, Mexico, 2015, and first confirmed transmission by *Aedes aegypti* mosquitoes in the Americas. *J Infect Dis.* (2016) [Epub ahead of print]; DOI: 10.1093/infdis/jiw302.
- Mlakar J, M Korva, N Tul, M Popovic, M Poljsak-Prijatelj, J Mraz, M Kolenc, K Resman Rus, T Vesnaver Vipotnik, et al. (2016). Zika virus associated with microcephaly. *N Engl J Med* 374:951–958.
- Iimura T and O Pourquie. (2008). Manipulation and electroporation of the avian segmental plate and somites *in vitro*. *Methods Cell Biol* 87:257–270.
- Boss A, M Oppitz, HF Wehrl, C Rossi, M Feuerstein, CD Claussen, U Drews, BJ Pichler and F Schick. (2008). Measurement of T₁, T₂, and magnetization transfer properties during embryonic development at 7 Tesla using the chicken model. *J Magn Reson Imaging* 28:1510–1514.
- de Fatima Vasco Aragao M, V van der Linden, AM Brainer-Lima, RR Coeli, MA Rocha, P Sobral da Silva, M Durce Costa Gomes de Carvalho, A van der Linden, A Cesario de Holanda and MM Valenca. (2016). Clinical features and neuroimaging (CT and MRI) findings in presumed Zika virus related congenital infection and microcephaly: retrospective case series study. *BMJ* 353: i1901.
- Driggers RW, CY Ho, EM Korhonen, S Kuivanen, AJ Jaaskelainen, T Smura, A Rosenberg, DA Hill, RL DeBiasi, et al. (2016). Zika virus infection with prolonged maternal viremia and fetal brain abnormalities. *N Engl J Med* 374: 2142–2151.
- Lazear HM, J Govero, AM Smith, DJ Platt, E Fernandez, JJ Miner and MS Diamond. (2016). A mouse model of Zika virus pathogenesis. *Cell Host Microbe* 19:720–730.
- Calvet G, RS Aguiar, AS Melo, SA Sampaio, I de Filippis, A Fabri, ES Araujo, PC de Sequeira, MC de Mendonca,

- et al. (2016). Detection and sequencing of Zika virus from amniotic fluid of fetuses with microcephaly in Brazil: a case study. *Lancet Infect Dis* 16:653–660.
18. Hanners NW, JL Eitson, N Usui, RB Richardson, EM Wexler, G Konopka and JW Schoggins. (2016). Western Zika virus in human fetal neural progenitors persists long term with partial Cytopathic and Limited Immunogenic Effects. *Cell Rep* 15:2315–2322.
 19. Kleber de Oliveira W, J Cortez-Escalante, WT De Oliveira, GM do Carmo, CM Henriques, GE Coelho and GV Araujo de Franca. (2016). Increase in reported prevalence of microcephaly in infants born to women living in areas with confirmed Zika virus transmission during the first trimester of pregnancy—Brazil, 2015. *MMWR Morb Mortal Wkly Rep* 65:242–247.
 20. Tsai HM, BB Garber and LM Larramendi. (1981). 3H-thymidine autoradiographic analysis of telencephalic histogenesis in the chick embryo: I. Neuronal birthdates of telencephalic compartments in situ. *J Comp Neurol* 198:275–292.
 21. Paploski IA, AP Prates, CW Cardoso, M Kikuti, MM Silva, LA Waller, MG Reis, U Kitron and GS Ribeiro. (2016). Time lags between exanthematous illness attributed to Zika virus, Guillain-Barre Syndrome, and Microcephaly, Salvador, Brazil. *Emerg Infect Dis* 22:1438–1444.
 22. Miner JJ, A Sene, JM Richner, AM Smith, A Santeford, N Ban, J Weger-Lucarelli, F Manzella, C Ruckert, et al. (2016). Zika virus infection in mice causes panuveitis with shedding of virus in tears. *Cell Rep* 16:3208–3218.
 23. Slotkin TA, FJ Seidler, IT Ryde and J Yanai. (2008). Developmental neurotoxic effects of chlorpyrifos on acetylcholine and serotonin pathways in an avian model. *Neurotoxicol Teratol* 30:433–439.
 24. Cugola FR, IR Fernandes, FB Russo, BC Freitas, JL Dias, KP Guimaraes, C Benazzato, N Almeida, GC Pignatari, et al. (2016). The Brazilian Zika virus strain causes birth defects in experimental models. *Nature* 534:267–271.
 25. Zhou Z, Z Chen, J Shan, W Ma, L Li, J Zu and J Xu. (2015). Monitoring brain development of chick embryos in vivo using 3.0 T MRI: subdivision volume change and preliminary structural quantification using DTI. *BMC Dev Biol* 15:29.
 26. Hazin AN, A Poretti, CM Turchi Martelli, TA Huisman; Microcephaly Epidemic Research Group, D Di Cavalcanti Souza Cruz, M Tenorio, A van der Linden, LJ Pena, et al. (2016). Computed tomographic findings in microcephaly associated with Zika virus. *N Engl J Med* 374:2193–2195.
 27. Wu KY, GL Zuo, XF Li, Q Ye, YQ Deng, XY Huang, WC Cao, CF Qin and ZG Luo. (2016). Vertical transmission of Zika virus targeting the radial glial cells affects cortex development of offspring mice. *Cell Res* 26:645–654.
 28. Rossi SL, RB Tesh, SR Azar, AE Muruato, KA Hanley, AJ Auguste, RM Langsjoen, S Paessler, N Vasilakis and SC Weaver. (2016). Characterization of a novel murine model to study Zika virus. *Am J Trop Med Hyg* 94:1362–1369.
 29. Dudley DM, MT Aliota, EL Mohr, AM Weiler, G Lehrer-Brey, KL Weisgrau, MS Mohns, ME Breitbach, MN Rashed, et al. (2016). A rhesus macaque model of Asian-lineage Zika virus infection. *Nat Commun* 7:12204.
 30. Ramos da Silva S and SJ Gao. (2016). Zika virus: an update on epidemiology, pathology, molecular biology, and animal model. *J Med Virol* 88:1291–1296.
 31. Palacios R, GA Poland and J Kalil. (2016). Another emerging arbovirus, another emerging vaccine: targeting Zika virus. *Vaccine* 34:2291–2293.

Address correspondence to:

*Dr. Melinda A. Brindley
Department of Infectious Diseases, Population Health
Center for Vaccines and Immunology
College of Veterinary Medicine
University of Georgia
Athens, GA 30602*

E-mail: mbrindle@uga.edu

Received for publication July 30, 2016

Accepted after revision September 13, 2016

Prepublished on Liebert Instant Online September 14, 2016